

An Ab initio Study of the P–C Bond Rotation in Phosphoryl- and Thiophosphoryl-Stabilized Carbanions: Five- and Six-Membered Heterocycles

Michael Kranz, Scott E. Denmark,* Kevin A. Swiss, and Scott R. Wilson

Roger Adams Laboratory, University of Illinois, Urbana–Champaign, 600 South Mathews Avenue, Urbana, Illinois 61801

Received February 9, 1996 (Revised Manuscript Received September 18, 1996[®])

The potential energy surfaces for the P–C bond rotation in the 2-oxo- and 2-thioxo-2-methyl-1,3,2-diazaphosphorinane and -1,3,2-diazaphospholidine anions have been investigated at MP4(SDQ)/6-31+G*//HF/6-31+G* + ZPE. Four stationary points have been found for the six-membered ring species. The lowest energy structures exhibit a completely or nearly planar carbanion with its substituents parallel to the P=X axis (X = O, S). The transition state (TS) structures have a strongly pyramidalized carbanion in which the lone pair (LP) is approximately perpendicular to the P=X bond. Isodesmic equations, bond length comparisons, and orbital interactions indicate a superior ground state (GS) stabilization of the thioxo derivative and a favorable TS stabilization of the oxo species. Both effects cooperate to furnish the computationally and experimentally observed higher (ca. 2.5 kcal/mol in both cases) P–C rotational barrier for the 2-thioxo-1,3,2-diazaphosphorinane based anions. Coordination of a lithium cation to the chalcogen atom yields a distinct preference for the axial/equatorial orientation of the nitrogen substituents in the oxo species and for the diequatorial arrangement in the thioxo analog, in perfect agreement with X-ray crystallographic data. The X-ray crystal structure of lithio 2-(1-methylethyl)-1,3-dimethyl-1,3,2-diazaphosphorinane 2-sulfide·3THF is reported and it is consistent with existing theoretical and experimental geometries. The five-membered ring analogs (1,3,2-diazaphospholidines) exhibit the same conformational preference for the carbanion in the GS and the TS. The activation barrier for P–C bond rotation is higher in the thioxo derivatives as well. Whereas only one nitrogen substituent changes its orientation in the diazaphosphorinanes during the P–C rotational coordinate, the ring backbone responds strongly in the diazaphospholidines.

Introduction

As part of a broadly-based program on the synthetic applications of asymmetrically modified phosphorus(V)-stabilized carbanions,¹ we have undertaken a thorough examination of the structures of these species. One of the more intriguing dimensions of this program has been the comparison of phosphoryl (P=O)- versus thiophosphoryl (P=S)-type anion-stabilizing groups. To complement ongoing studies and provide a foundation for the fundamental understanding of the relationship between structure and reactivity of phosphorus(V)-stabilized carbanions, we have initiated a comparison of phosphoryl- and thiophosphoryl-stabilized anions by computational methods. The basic features of bonding, hybridization, and rotational barriers in simple, acyclic phosphorus(V) derivatives have been detailed in an earlier account.² Herein we describe an expanded computational examination of the synthetically more significant cyclic phosphonamides and thiophosphonamides in five- and six-membered rings.

Background

Preparative. In the early stages of our search for a general and highly selective chiral auxiliary for phosphorus(V) anionic reagents, we noted a strong dependence of reaction selectivity on many structural variables such as heterocycle ring size, P=O versus P=S stabiliza-

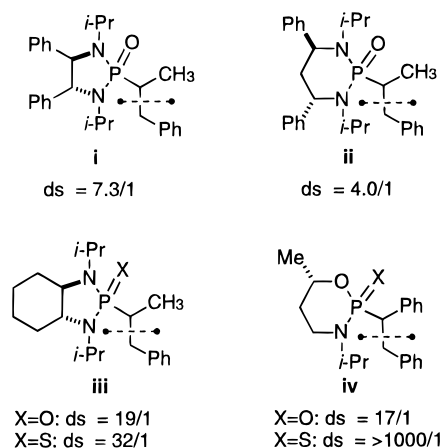


Figure 1. Comparison of alkylation selectivities for various types of auxiliaries.

tion, nature of the nitrogen substituent, nature of the carbanion, and the electrophile. A selection of these results, which highlights the importance of ring size and anion-stabilizing group (constant N-substituent, and alkylating agent), is compiled in Figure 1. While the change in diastereoselectivity between phospholidine **i** and phosphorinane **ii** is noteworthy, a much greater effect is observed with the rigid phospholidine **iii**.³ Most striking, however, is the enhancement in diastereoselectivity of benzylation in **iii** and **iv**⁴ when changing from

[®] Abstract published in *Advance ACS Abstracts*, November 1, 1996.
 (1) Denmark, S. E.; Chen, C.-T.; Reed, R. A. *Adv. Carbanion Chem.* Manuscript in preparation.
 (2) Kranz, M.; Denmark, S. E. *J. Org. Chem.* **1995**, *60*, 5867.

(3) (a) Denmark, S. E.; Kim, J.-H. *J. Org. Chem.* **1995**, *60*, 7535.
 (b) Denmark, S. E.; Kim, J.-H.; Pansare, S. V. Manuscript in preparation.
 (c) Brice, L. J. Unpublished results from these laboratories.
 (4) Denmark, S. E.; Chen, C.-T. *J. Am. Chem. Soc.* **1995**, *117*, 11879.

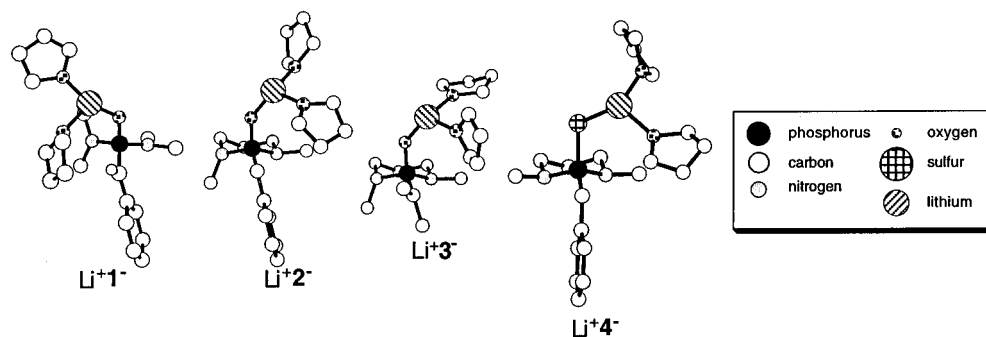


Figure 2. X-ray structures of P=O- (Li^+1^- , Li^+2^- , and Li^+3^-) and P=S-stabilized (Li^+4^-) anions.

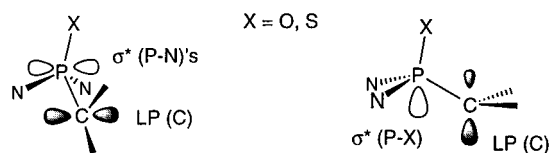
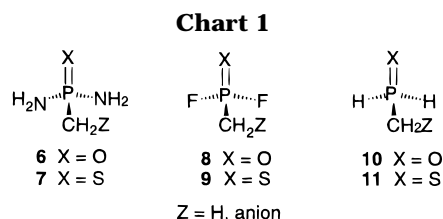


Figure 3. Simplified representation of the electron distribution of the lone pair on carbon in the GS and TS and the estimated shape of the respective major stabilizing orbital.

P=O- to P=S-stabilized anions. The origins of these differences clearly must reside in the changes in anion structure, conformation, and rotational dynamics in response to the alterations in steric and electronic influences as provided by the shape and nature of the stabilizing group.

Structural. The solution- and solid-state structures of cyclic and acyclic phosphoryl- and thiophosphoryl-stabilized anions reveal important clues that clarify the differences and similarities between these families of organolithium compounds. The X-ray crystallographic structures of three lithiated oxophosphoryl (Li^+1^- ,^{5a} Li^+2^- ,^{5b} Li^+3^- ^{5c}) and one thiophosphoryl diamide system (Li^+4^-)^{6a} display these characteristics in common (Figure 2): (1) the lithium cation is always bonded to the chalcogen on phosphorus and has no contact with the carbanion, (2) the carbanionic center is almost or completely planar, (3) the carbanion is oriented parallel to the P=X bond (X = O, S) or nearly so, and (4) all of these anions crystallize as dimers with two THF molecules on each lithium.

Variable-temperature solution NMR experiments have also provided an activation barrier for the P–C bond rotation in the Li^+3^- ($\Delta G^\ddagger(\text{Me}_2\text{O}) = 6.7 (\pm 0.6) \text{ kcal/mol}$)^{5a} and in the thiophosphoryl analog Li^+5^- ($\Delta G^\ddagger(\text{THF}) = 9.8 (\pm 0.3) \text{ kcal/mol}$),^{6b} the X-ray crystal structure of which will be reported herein.

Theoretical. Schleyer, Houk, et al. have reported a comprehensive (albeit computationally rudimentary) survey of heteroatom substituent effects on carbanion stability.⁷ They established that the superior stabilizing effects of second-row compared to first-row elements have their origin in the greater ease of polarizability, the more

electropositive character, and the stronger tendency for negative hyperconjugation.

Of the computational approaches to phosphorus-stabilized carbanions,^{2,5a,8–10} the earlier studies partly suffered from basis set inadequacy while still providing valuable insights. Detailed examinations of the P–C bond rotation in phosphonic diamides (**6**, **7**, Chart 1) and difluorides (**8**, **9**) helped to visualize and quantify the objects of previous assumptions derived from experimental findings.^{2,5a} In the lowest energy structure, the carbanion lone pair orientation is computed to be perpendicular to the P=X axis in agreement with experiment (vide supra). Structural details and an isodesmic equation determine the P=S moiety to be superior to the P=O group in stabilizing a carbanion in the GS arrangement.¹¹ NBO analyses of the HF/6-31+G* wavefunction reveal the $\sigma^*(\text{P-N})$ orbitals to be better acceptors compared to the $\sigma^*(\text{P=X})$ orbital. Oxygen LP backbonding into the $\sigma^*(\text{P-N})$ orbitals leads to the diminished acceptor capabilities for the carbanion LP, thus raising the GS energy of the P=O species and decreasing its energy gap to the TS (Figure 3). The TS geometry exhibits a strongly pyramidalized carbanion antiperiplanar to the P=X group. In this arrangement, both chalcogens exert about the same stabilizing effect upon the carbanion. With less electronegative substituents on phosphorus (H (**10**, **11**) instead of NH_2 or F), the $\sigma^*(\text{P=X})$ orbital becomes a stronger LP acceptor than the $\sigma^*(\text{P-H})$ orbitals, changing the orientation of the carbanion in the GS and TS and inverting the P=O/S rotational barrier sizes.

Due to the freely rotating nitrogen substituents in the phosphonic diamides **6** and **7**, the P–C rotational barriers (P=O, 2.5 kcal/mol; P=S, 2.8 kcal/mol) are much lower than the NMR-determined values of their derivatives Li^+3^- and Li^+5^- (vide supra).² The activation energies for rotation come out higher if the nitrogen substituents

(5) (a) Cramer, C. J.; Denmark, S. E.; Miller, P. C.; Dorow, R. L.; Swiss, K. A.; Wilson, S. R. *J. Am. Chem. Soc.* **1994**, *116*, 2437. (b) Denmark, S. E.; Dorow, R. L. *J. Am. Chem. Soc.* **1990**, *112*, 864. (c) Denmark, S. E.; Miller, P. C.; Wilson, S. R. *J. Am. Chem. Soc.* **1991**, *113*, 1468.

(6) (a) Denmark, S. E.; Swiss, K. A.; Wilson, S. R. *J. Am. Chem. Soc.* **1993**, *115*, 3826. (b) Denmark, S. E.; Swiss, K. A. *J. Am. Chem. Soc.* **1993**, *115*, 12195.

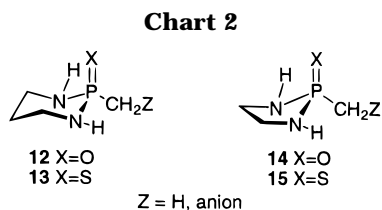
(7) (a) Schleyer, P. v. R.; Clark, T.; Kos, A. J.; Spitznagel, G. W.; Rohde, C.; Arat, D.; Houk, K. N.; Rondan, N. G. *J. Am. Chem. Soc.* **1984**, *106*, 6467. See also: (b) Bernardi, F.; Bottoni, A.; Valli, G. S.; Venturini, A. *Gazz. Chim. Ital.* **1990**, *120*, 301. (c) El-Nahas, A. M.; Schleyer, P. v. R. *J. Comput. Chem.* **1994**, *15*, 596.

(8) Streitwieser, A., Jr.; Rajca, A.; McDowell, R. S.; Glaser, R. *J. Am. Chem. Soc.* **1987**, *109*, 4184.

(9) Denmark, S. E.; Cramer, C. J. *J. Org. Chem.* **1990**, *55*, 1806.

(10) Zarges, W.; Marsch, M.; Harms, K.; Haller, F.; Frenking, G.; Boche, G. *Chem. Ber.* **1991**, *124*, 861.

(11) For a review of the bonding in phosphoryl and thiophosphoryl compounds, see: Gilheany, D. G. *Chem. Rev.* **1994**, *94*, 1339.



are fixed during rotation and even more if, in addition, a lithium cation is coordinated to the phosphoryl oxygen.^{5a}

Instead of artificially constraining the geometries of the acyclic phosphonic diamides, we set out to investigate the actual ring compounds lacking only their methyl groups on the nitrogens and the deprotonated carbons. The 1,3,2-diazaphosphorinane system (**12**, **13**) has been chosen due to the wealth of structural information accumulated for its derivatives, and the 1,3,2-diazaphospholidine (**14**, **15**) can be viewed as a mimic for the conformationally more constrained octahydrobenzodiazaphosphole (**iii**). A search for appropriate basis sets for the acyclic compounds has previously been performed.²

The goals of the study herein include the following: (1) evaluating the potential energy surface of six-membered ring phosphonic diamide **12**⁻ and thiophosphonic diamide **13**⁻ (Chart 2), along with the five-membered ring analogs **14**⁻ and **15**⁻, (2) determining the P–C rotational barriers for these molecules, (3) comparing the lithiated anions Li⁺**12**⁻ and Li⁺**13**⁻ to X-ray crystallographic data, and (4) tracing the origin of the stabilizing effects in these compounds by analyzing their wavefunctions. Finally, we also report a new X-ray crystal structure of a *monomeric* lithiated thiophosphoryl-stabilized anion.

To help visualize the features of carbanion structure and orientation, a systematic graphic description has been formulated below. The key attributes that characterize the carbanion geometry are its torsion with respect to the P=X bond (α) and its degree of pyramidalization (β), Figure 4. These angles are defined by creating an imaginary reference plane that bisects the H–C–H angle. The angle α describes the torsion between the P=X axis and this plane ($|\alpha| \leq 90^\circ$). The angle β is defined between one of the carbanion hydrogens and the plane such that $|\beta| \geq 90^\circ$. In this way, (1) the hybridization of the carbanion is easily deduced from the limits, $90^\circ = sp^2$ and $120^\circ = sp^3$, and (2) an inversion of the carbanion is accompanied by a change in the sign of the β value. The pyramidalization of the nitrogen atoms is indicated by the sum of angles at this atom. Herein, the limits of pyramidalization are defined by $360^\circ = sp^2$ and $327^\circ = sp^3$.

Methods

Computational. Standard basis sets¹² incorporated into the Gaussian92 program¹³ were employed on an SGI Power Challenge at the National Center of Supercomputing Applications at Urbana–Champaign. All geometries were fully optimized within the designated symmetry constraints with the restricted Hartree–Fock (RHF)¹⁴ method. Further correction for electron correlation was introduced by single point

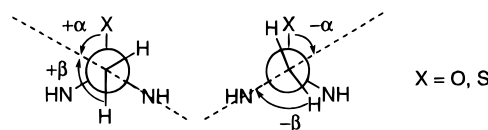


Figure 4. Definition for α and β angles (view along P–C bond).

calculations at the fourth-order Møller–Plesset (MP4)¹⁵ perturbation theory. Analytical frequency analyses were carried out to characterize stationary points and to obtain zero point vibrational energies (ZPE), which were scaled by 0.89¹⁶ to calculate the final energy estimates. The wavefunctions obtained at RHF/6-31+G* were analyzed with the natural bond orbital (NBO) method¹⁷ included in Gaussian92. Hyperconjugative effects can be assessed by use of the second order perturbation theory.¹⁸ Although this procedure is known to overestimate stabilizing interactions, they closely parallel the energies attained by the more accurate Fock matrix deletion procedure.¹⁹

Experimental. For a recent description of the general synthetic methods see ref 4. NMR data are reported in ppm; coupling constants are in Hz; IR data are in cm^{-1} ; mass spectral data are given as m/z .

2-(1-Methylethyl)-1,3-dimethyl-1,3,2-diazaphosphorinane 2-Sulfide (5). A 250-mL, three-necked flask was charged with (1-methylethyl)thioxophosphonic dichloride²⁰ (7.88 g, 44 mmol), dichloromethane (180 mL), and triethylamine (20 mL, 150 mmol, 3.4 equiv). To this solution was slowly added *N,N*-dimethyl-1,3-propanediamine (5.0 g, 49 mmol, 1.1 equiv) over 5 min. The reaction mixture was stirred for 16 h at rt and then was concentrated in vacuo. The white solid residue was filtered and washed with EtOAc (4 \times 30 mL). The filtrate and EtOAc washes were combined and concentrated by rotary evaporation to afford an oil that was purified by silica gel column chromatography (EtOAc/hexane, 3/1) to afford 7.92 g (88%) of **5**. Further purification by bulb-to-bulb distillation afforded 7.38 g (82%) of **5** as a colorless oil: bp 150 $^\circ C$ (0.3 Torr); mp $\sim 12^\circ C$ (solidifies); 1H NMR (400 MHz) 3.02 (dm, $^3J_{HP} = 13.4$, 4 H, $H_2C(4)$, $H_2C(6)$), 2.64 (d, $^3J_{HP} = 12.7$, 6 H, NCH_3), 2.36 (dq, $^2J_{HP} = 19.8$, $J_{HH} = 7.1$, 1 H, $(CH_3)_2CHP$), 1.85 (m, 1 H, $H_{ax}C(5)$), 1.79 (m, 1 H, $H_{eq}C(5)$), 1.19 (dd, $^3J_{HP} = 18.6$, $J_{HH} = 7.1$, 6 H, $(CH_3)_2CHP$); ^{13}C NMR (100.6 MHz) 49.43 (d, $^2J_{CP} = 2.8$, C(4,6)), 37.77 (d, $^2J_{CP} = 2.3$, NCH_3), 31.20 (d, $^1J_{CP} = 88.5$, $(CH_3)_2CHP$), 24.41 (d, $^3J_{CP} = 1.9$, C(5)), 17.09 (d, $^2J_{CP} = 1.9$, $(CH_3)_2CHP$); ^{31}P NMR (161.9 MHz) 94.94; IR (thin film) 2928 (s), 2812 (m), 1464 (m), 1377 (w), 1361 (w), 1306 (w), 1277 (m), 1223 (m), 1196 (w), 1157 (m), 1126 (m), 1047 (s), 1010 (m), 949 (m), 904 (m), 883 (m), 860 (s); MS (70 eV) 206 (M^+ , 5), 164 (7), 163 (100), 131 (27), 88 (11), 70 (9), 63 (9), 44 (15); TLC $R_f = 0.37$ (EtOAc/hexane, 3/1). Anal. Calcd for $C_8H_{19}N_2PS$ (206.287): C, 46.58; H, 9.28; N, 13.58; P, 15.01; S, 15.54. Found: C, 46.30; H, 9.11; N, 13.45; P, 14.88; S, 15.36.

Lithio 2-(1-Methylethyl)-1,3-dimethyl-1,3,2-diazaphosphorinane 2-Sulfide (Li⁺5**⁻).** 2-(1-Methylethyl)-1,3-dimethyl-1,3,2-diazaphosphorinane-2-sulfide (724.7 mg, 3.5 mmol) was introduced into a flame-dried 10-mm NMR tube fitted with a rubber septum and a nitrogen inlet (syringe needle). Anhydrous THF (2.3 mL) was added via syringe, and the solution was cooled in a $-78^\circ C$ bath. *n*-Butyllithium (350 μL , 10 M, 3.5 mmol) was added dropwise via syringe (final anion concn ~ 1.5 M). The yellow solution was stored at $-78^\circ C$ overnight to give clear colorless crystals that melt near $-50^\circ C$. For the crystal mounting and diffraction experimental details, see the supporting information.

(12) Hehre, W. J.; Radom, L.; Schleyer, P. v. R.; Pople, J. A. *Ab Initio Molecular Orbital Theory*; Wiley-Interscience: New York, 1986.

(13) Gaussian92, Revision E2 and G3. Frisch, M. J.; Trucks, G. W.; Head-Gordon, M.; Gill, P. M. W.; Wong, M. W.; Foresman, J. B.; Johnson, B. G.; Schlegel, H. B.; Robb, M. A.; Replogle, M. S.; Gomperts, R.; Andres, J. L.; Raghavachari, K.; Binkley, J. S.; Gonzalez, C.; Martin, R. L.; Fox, D. J.; Defrees, D. J.; Baker, J.; Stewart, J. J. P.; Pople, J. A. Gaussian, Inc., Pittsburgh, PA, 1992.

(14) Roothaan, C. C. J. *Rev. Mod. Phys.* **1951**, *23*, 69.

(15) (a) Møller, C.; Plesset, M. S. *Phys. Rev.* **1934**, *46*, 618. (b) Binkley, J. S.; Pople, J. A. *Int. J. Quant. Chem.* **1975**, *9*, 229.

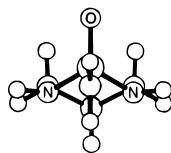
(16) Pople, J. A.; Krishnan, R.; Schlegel, H. B.; Binkley, J. S. *Int. J. Quant. Chem.* **1979**, *13*, 225.

(17) (a) Glendening, E. D.; Reed, A. E.; Carpenter, J. E.; Weinhold, F. *NBO Version 3.1*. (b) Reed, A. E.; Curtiss, L. A.; Weinhold, F. *Chem. Rev.* **1988**, *88*, 899.

(18) Tyrrell, J.; Weinstock, R. B.; Weinhold, F. *Int. J. Quant. Chem.* **1981**, *19*, 781.

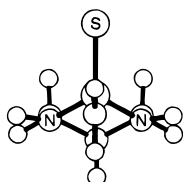
(19) Arnaud, R. *J. Comput. Chem.* **1994**, *15*, 1341.

(20) Kaushik, M. P.; Vaidyanathaswamy, R. *J. Org. Chem.* **1980**, *45*, 2270.

Table 1. Coordinate for the P–C Bond Rotation in 12⁻ at 3-21G*

α^a (deg)	rel energy (kcal/mol)	β (deg)	Σ angles N(1)/N(2) (deg)
90	0.0	90	347/347
75	+0.48	93.4	346/346
60	+2.05	95.5	344/347
45	+4.69	95.8	342/348
30	+3.18	-93.3	342/342
15	+4.70	-100.9	344/341
0	+5.60	-104.0	347/340

^a See Figure 4 for definition.

Table 2. Coordinate for the P–C Bond Rotation in 13⁻ at 3-21G*

α (deg)	rel energy (kcal/mol)	β (deg)	Σ angles N(1)/N(2) (deg)
90	0.0	90	347/347
75	+0.68	92.6	347/347
60	+2.78	94.3	346/347
45	+6.26	94.4	345/348
30	+7.16	-99.6	344/345
15	+8.90	-107.6	345/343
0	+9.93	-110	347/343

Results and Discussion

Rotational Coordinates of the 2-Methyl-1,3,2-Diazaphosphorinane 2-Oxide (12⁻) and 2-Sulfide (13⁻) Anions. The structural changes that accompany incremental (15°) P–C bond rotation in 12⁻ and 13⁻ were calculated at the HF/3-21G* level (Tables 1 and 2). Both molecules undergo almost identical changes in conformation during the rotation, however, the magnitude of concomitant changes in energy differs: the thioxo derivative 13⁻ arrives at nearly twice the relative energy (+9.9 kcal/mol) at the highest point of the rotational coordinate than does 12⁻ (+5.6 kcal/mol).

The anions 12⁻ and 13⁻ display the following common characteristics: (1) the minimum structure exhibits a perfectly planar carbanion ($\beta = 90^\circ$) that is oriented parallel to the P=X axis ($\alpha = 90^\circ$), (2) in this structure both N–H's assume equatorial positions at the slightly pyramidalized nitrogens, thus rendering C_s symmetric molecules, and (3) there is no visible change in the disposition of the backbone hydrogens or the N–H's during P–C bond rotation through $\alpha = 45^\circ$. At this point, the relative energy for 13⁻ is only 1.6 kcal/mol higher than for 12⁻. The most notable geometrical change that takes place in either series occurs during the next rotational increment to $\alpha = 30^\circ$. The initially symmetric lone pair (LP) on carbon becomes polarized in a way to avoid the unfavorable σ (P–N) bond overlap and to increase interaction with the σ^* orbital of the same bond. The carbon LP axis points toward one of the formerly axially disposed nitrogen LP's. As a consequence, this nitrogen atom now inverts to avoid the unfavorable LP–

LP interaction, thus placing the hydrogen atom in an axial orientation. In concert with the nitrogen inversion is the inversion of the anionic carbon (cf. β angles), which points the carbon LP away from the σ (P=X) bond and increases the interaction with the attendant σ^* orbital. It is at this point ($\alpha = 30^\circ$) that the greatest difference between the two chalcogen derivatives is found; while the relative energy for the oxo analog 12⁻ drops to +3.2 kcal/mol, it rises to +7.2 kcal/mol for 13⁻. During the last two rotational increments, the only geometrical change in either series is the increasing carbon pyramidalization that eventually yields a CH₂ group oriented pseudoperpendicularly to the P=X axis. In addition, this structure displays equatorially/axially disposed N–H's at the highest energy point of the rotational coordinate ($\alpha = 0^\circ$). The thioxo analog 13⁻ finishes 4.3 kcal/mol higher than does the oxo counterpart 12⁻.

There are distinct differences between these geometries and those of both acyclic phosphonic diamides (6⁻, 7⁻) in the HF/3-21G* rotational coordinates.^{2,5a} The orientation of the anionic methylene group (α values) is reversed at the starting (relative energy = 0 kcal/mol) and ending points. This is most likely a consequence of the orientation and planarity of the nitrogen atoms in 6⁻ and 7⁻. In addition, the constraints on the disposition of the LP's in the ring limit their response to the orientation of the carbon LP. The change in energy during P–C bond rotation in 6⁻, 7⁻, and 12⁻ is cosine-shaped, whereas a steady increase is found in 13⁻, which must be related to the inferior stabilizing interactions for the respective geometries in 13⁻ (vide infra).

Stationary Points for the 2-Methyl-1,3,2-Diazaphosphorinane 2-Oxide Anion (12⁻). Two views of the four stationary points of 12⁻ at HF/6-31+G* along with structural parameters are given in Figure 5. In accord with the rotational coordinate geometry of 12⁻, the lowest energy minimum exhibits C_s symmetry, a planar carbanion parallel to the P=O axis, and pyramidal nitrogens with two equatorial N–H's. The equivalent structure of 6⁻ is not a stationary point at HF/6-31+G*.²

The geometry corresponding to the drop in energy at $\alpha = 30^\circ$ in the rotational coordinate optimizes into a C_1 minimum with $\alpha = 69^\circ$, which is only 0.15 kcal/mol above the global minimum structure. In the C_1 minimum, the carbanion is pyramidal ($\beta = 104^\circ$) (one of the hydrogens is oriented gauche to the P=O axis) and the NH's are axially/equatorially oriented. This structure embodies the familiar "pinwheel" arrangement of groups that was found to be characteristic of the global minimum of 6⁻ at $\alpha = 72^\circ$.^{2,5a} The degree of pyramidalization of the carbanion is identical for both molecules, but the LP orientation at one of the two nitrogens is different. The difference in bond lengths around the phosphorus atom can easily be rationalized by considering the different orientation of the nitrogen LP's.

A third, somewhat higher (+1.9 kcal/mol) minimum of 12⁻ has been located in which both N–H's are axially oriented, and it is thus C_s symmetric. The CH₂ group is pseudoperpendicular to the P=O axis and strongly pyramidalized ($\beta = -115.4^\circ$). The equivalent C_s minimum at the potential energy surface of 6⁻ exhibits very similar structural features.

The TS structure for the P–C bond rotation of 12⁻ at HF/6-31+G* is closely related to the last point on its rotational coordinate. This structure features a strongly pyramidalized carbanion which points its LP midway between the σ (P–N) and the σ^* (P=O) orbital along with

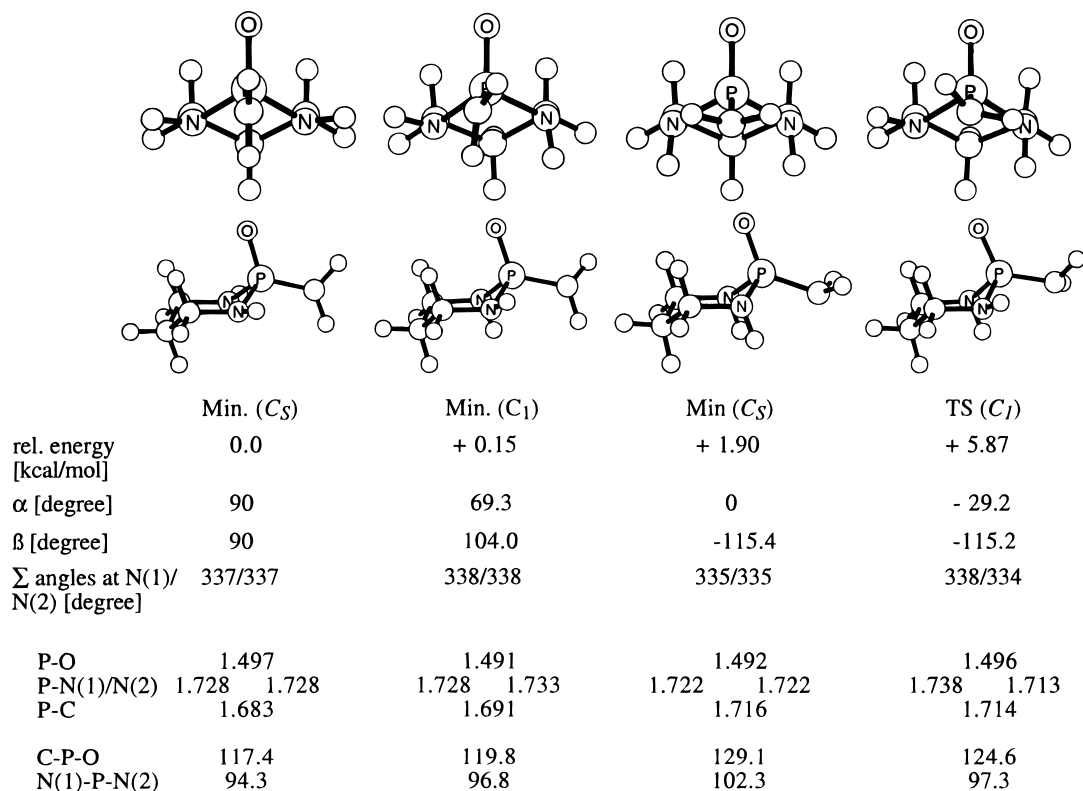


Figure 5. Stationary points for 12^- at MP4(SDQ)/6-31+G**/HF/6-31+G* (+ZPE).

axially/equatorially oriented N–H's. It is distinctly different from the TS of 6^- in that none of the carbon and nitrogen LP's is antiparallel to a neighboring bond as are all three LP's found in 6^- . The computed rotational barrier of 6^- has been shown to increase by about 1 kcal/mol upon lithium complexation of the oxygen in a fixed orientation.^{5a} Adding such an increment to the calculated activation barrier for 12^- (+5.9 kcal/mol) would then bring it very close to the NMR-determined value for the lithium salt of the *P*-(1-methylethyl)-*N,N*-dimethyl derivative of 12^- in THF ($\Delta G^\ddagger = 6.7$ kcal/mol).^{5a,c}

The experimental relevance of the calculated minimum structure of 12^- may be assessed by comparison to the X-ray crystal structure of lithio 2-(1-methylethyl)-1,3-dimethyl-1,3,2-diazaphosphorinane 2-oxide·2 THF (Li^+3^-)^{6c} (Figure 2). Overall, the gas phase calculations of a truncated derivative of Li^+3^- compare remarkably well with our X-ray data, which suggests that the geometry-determining effects are electronic in nature. Li^+3^- contains a slightly pyramidalized carbanion with its substituents gauche to the P=O axis. The nitrogen substituents are axially/equatorially oriented. These characteristics are strikingly similar to the C₁ minimum of 12^- , which is energetically almost degenerate with the global minimum. A full comparison will await discussion of the calculated structure of the lithiated anion (Li^+12^-) below.

Stationary Points for the 2-Methyl-1,3,2-Diazaphosphorinane 2-Sulfide Anion (13^-). A related set of stationary points for 13^- with structural characteristics (HF/6-31+G*) very similar to those for 12^- have been found (Figure 6). Despite the structural similarities, the relative energy differences among the rotamers of 13^- are larger, and the P–C and P–N bond lengths are almost always shorter in the thioxo analog as will be discussed below.

The global energy minimum for 13^- (2.0 kcal/mol lower than the second lowest structure) embodies the following: (1) a perfectly planar carbanion that is parallel to the P=S axis and (2) pyramidal nitrogens with equatorially disposed N–H's. The key features of this structure are remarkably well reflected in the X-ray crystal structure of lithio 2-benzyl-1,3-dimethyl-1,3,2-diazaphosphorinane 2-sulfide (Li^+4^-)^{6a} and in the solid state structure of Li^+5^- introduced below. The global minimum of 13^- has its equivalent on the potential energy surface of thioxophosphonic diamide (7^-) with very similar structural parameters, but the latter is a TS at HF/6-31+G* for the rotation of the amino groups. In both geometries of 13^- , the C₃ minimum with its N–H's axial and the TS structure with equatorial/axial N–H's, the anionic CH₂ group is polarized away from the P=S axis. These structures are 3.8 and 2.4 kcal/mol higher in relative energies than their oxo analogs, respectively. The larger P–C rotational barrier of 13^- (+8.3 kcal/mol) is in good agreement with the experimentally determined (NMR) barrier for lithio 2-(1-methylethyl)-1,3-dimethyl-1,3,2-diazaphosphorinane 2-sulfide (Li^+5^-) in THF ($\Delta G^\ddagger = 9.2$ kcal/mol).^{6a} Again, this number exceeds the computational value by 1 kcal/mol, ostensibly due to the missing lithium counterion (vide supra).^{6a}

Comparison between the *P*-Oxo and *P*-Thioxo Six-Membered Heterocycles. The differences in geometry between structures 12^- and 13^- are subtle. To evaluate the geometrical and energetic changes upon deprotonation, the neutral precursors of 12^- ($12H$) and 13^- ($13H$) have been optimized (Tables 3 and 4). The energy ordering of the three conformers is the same for both chalcogens: the diequatorial N–H orientation is lowest in energy followed by equatorial/axial and axial/axial. The computational results are supported by the

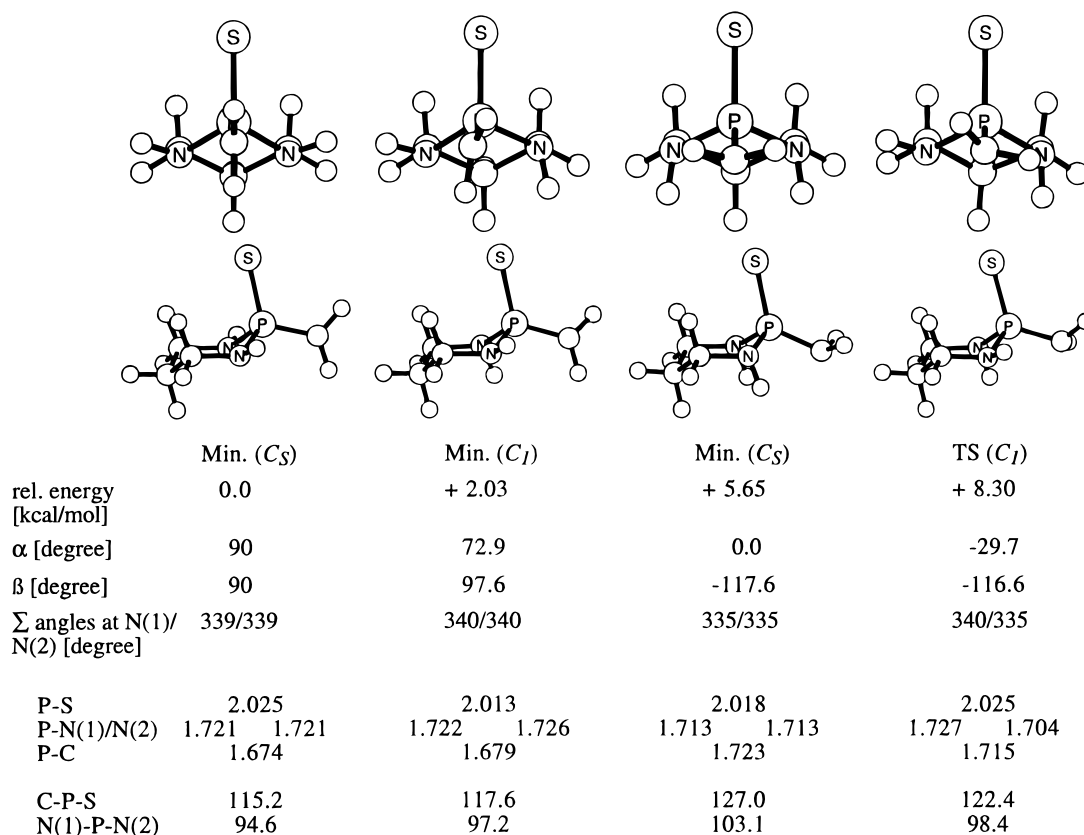


Figure 6. Stationary points for 13^- at MP4(SDQ)/6-31+G*/HF/6-31+G*(+ZPE).

Table 3. Stationary Points for 12H at MP4(SDQ)/6-31+G*/HF/6-31+G* (+ZPE)

	min (C_5)	min (C_1)	min (C_5)	X-ray structures ^a
N-Me orientation	eq/eq	eq/ax	ax/ax	
rel energy (kcal/mol)	0.0	+1.46	+4.91	
Σ angles at N(1)/N(2) (deg)	342/342	339/339	339/339	352-60
P-O (Å)	1.471	1.468	1.464	1.47-1.49
P-N(1) (Å)	1.678	1.689	1.685	1.62-1.69
P-N(2) (Å)	1.678	1.675	1.685	1.62-1.69
P-C (Å)	1.806	1.804	1.803	1.75-1.83
C-P-O (deg)	111.7	114.2	116.3	107-112
N-P-N (deg)	100.3	101.6	104.6	103-107

^a Range of data from Cambridge Crystallographic Database (five structures, ref 22a).

Table 4. Stationary Points for 13H at MP4(SDQ)/6-31+G*/HF/6-31+G* (+ZPE)

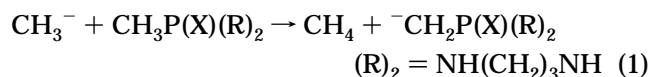
	min (C_5)	min (C_1)	min (C_5)	X-ray structures ^a
N-Me orientation	eq/eq	eq/ax	ax/ax	
rel energy (kcal/mol)	0.0	+1.71	+5.75	
Σ angles at N(1)/N(2) (deg)	340/340	338/339	339/339	341-60
P-S (Å)	1.963	1.956	1.950	1.93-1.96
P-N(1) (Å)	1.682	1.692	1.688	1.63-1.69
P-N(2) (Å)	1.682	1.677	1.688	1.63-1.69
P-C (Å)	1.809	1.809	1.809	1.77-1.85
C-P-S (deg)	112.9	114.4	115.8	108-116
N-P-N (deg)	100.1	101.6	104.5	104-110

^a Range of data from Cambridge Crystallographic Database (seven structures, ref 22b).

diequatorial orientation of the *N*-methyl groups found in the X-ray crystal structure of **4H**.²¹ The bond lengths around phosphorus in **12H** and **13H** are in the range of the values obtained from X-ray crystallographic data.²² The significant degree of nitrogen pyramidalization is

much stronger than in most phosphonic diamides in the solid state, but the wide range of experimental data hints to a shallow energy potential for this deformation.

The most appropriate acceptor orbitals for the carbon LP in the GS structures of 12^- and 13^- are the σ^* (P-N) orbitals. This electron delocalization causes a P-N bond lengthening and a P-C bond shortening compared to the protonated species.^{5,7,11} The concomitant P=X bond lengthening has been attributed to electrostatic repulsion between the carbanion and the chalcogen⁸ and to a diminished chalcogen LP back bonding into the σ^* (P-N) orbitals.^{2,11} As in the acyclic systems **6**⁻ and **7**⁻, the P-C bond shortens more in the thioxo than in the oxo case, reflecting the superior anion-stabilizing properties of the thiophosphoryl group.² These stabilization energies can be assessed by means of an isodesmic equation (eq 1) and turn out to be even larger than those of the acyclic phosphonic diamides (at the same level of theory: **6**⁻, -40 kcal/mol; **7**⁻, -47 kcal/mol). Without a chalcogen on phosphorus, the stabilizing effect is dramatically lower: PH_2 (QCISD(T)/6-31+G**/MP2/HF/6-31+G* + ZPE), -23 kcal/mol.^{7c}



MP4(SDQ)/6-31+G**/HF/6-31+G* + ZPE:

X = O: -42.2 kcal/mol
X = S: -49.6 kcal/mol

NBO Analysis. This localization procedure generates a P=C double bond for the two lowest energy structures of 12^- and 13^- , whereas for the other two geometries it produces a LP on the carbanion that strongly delocalizes

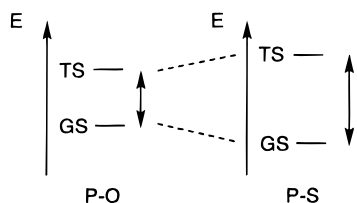


Figure 7. Schematic representation of the relative difference between the lowest minimum structure and the TS for **12⁻** and **13⁻**.

into adjacent σ^* orbitals. This difference is due to an arbitrarily fixed threshold in the NBO algorithm and limits comparisons to molecules with equivalent NBO pictures, although it does not affect the NBO atomic charges. The structural characteristics and thus the orbital interactions according to the NBO analysis are very similar for all the rotamers of **12⁻** and **13⁻** compared to those of **6⁻** and **7⁻**. A detailed bonding analysis has been given previously.²

The NBO atomic charges hardly change among the different rotamers. The charge on carbon is very similar in both molecules (**12⁻**, -1.46; **13⁻**, -1.40) but significantly different on phosphorus (**12⁻**, +2.40; **13⁻**, +1.86). The electrostatic attraction between the more positive phosphorus atom in **12⁻** and its negatively charged neighbors is much stronger than in **13⁻**. On the other hand, the stronger LP back bonding from oxygen into σ^* (P-N), σ^* (P-C), and π^* (P-C) orbitals in **12⁻** renders them less available for stabilization of the negative charge compared to the analogous interactions with sulfur in **13⁻**. These interactions give rise to the following structural consequences: (1) the differential occupation in the σ^* (P-N) orbitals affects the P-C bond length most in the two lower energy minima (parallel orientation of carbanion and P=X axis): the P-C bond is 0.01 Å shorter in **13⁻** in those two rotamers; (2) in contrast, the P-C bond is longer in **13⁻** in the second C_s minimum (pseudoperpendicular orientation of carbanion and P=X axis): the carbon LP delocalizes into the σ^* (P=X) orbital to an equal extent in both chalcogens but the stronger electrostatic P-C attraction in **12⁻** dominates; and (3) in the TS, the carbanion orientation is between the two previously described cases, which leads to almost identical P-C bond lengths in **12⁻** and **13⁻**. In accord with the confluent electronic and structural characteristics of the phosphorinanes and the acyclic phosphonic diamides, our previous conclusions also apply: the carbanion is better stabilized in the GS structure of **13⁻** compared to **12⁻**, while in the TS structure the oxophosphoryl group renders the superior stabilization. Both of these effects conspire to yield a lower activation barrier for **13⁻** (Figure 7).²

X-ray Crystal Structure of Lithio 2-(1-Methyl-ethyl)-1,3-dimethyl-1,3,2-diazaphosphorinane 2-Sulfide·3THF (Li⁺5⁻). To provide additional structural information on thiophosphonamide anions, our interest turned to defining the solid state structure of Li⁺5⁻, a compound that had been extensively studied in solution.

(22) A search of the Cambridge Crystallographic Database (version 3.21) located 12 examples of phosphonic di(bisalkyl)amides and seven of thioxophosphonic di(bisalkyl)amides. The phosphorus-bound carbon atoms in the acyclic structures are sp^2 hybridized. (a) P=O acyclic: DOKZEL, JISYIT, JISYOZ, OMAPBD, VIJNOR. (b) P=S acyclic: DODDLJ, JEXJUR, KETJAU, KICFEH, PAFKUC, VEZKIU, YAGLOH. (c) P=O five ring cyclic: CUXDII, DOCSAK, JECYIZ, JOTFIH, JOTFON, KADMOR, KIVFEA.

Table 5. Crystal and Experimental Data for Li⁺5⁻

crystal system	monoclinic
space group	$P2_1/n$
<i>a</i> , Å	11.934(8)
<i>b</i> , Å	13.077(10)
<i>c</i> , Å	16.111(9)
β , deg	93.22(5)
<i>V</i> , Å ³	2510(3)
<i>Z</i>	4
ρ (calcd), g/cm ³	1.134
temperature, °C	-100
color, habit	colorless, transparent, cubic
dimensions, mm	0.55, 0.45, 0.35
diffractometer	Enraf-Nonius CAD4 Mo K α
μ , cm ⁻¹	2.13
2 θ limit, deg (octants)	48.0 ($\pm h+k+l$)
intensities measd (unique)	4085 (3933)
intensities > 2 $\sigma(I)$	3895
<i>R</i>	0.067
wR2	0.152
density range in ΔF map, e/Å ³	+0.24 to -0.40

Table 6. Selected Bond Lengths, Bond Angles, and Nonbonded Distances for Li⁺5⁻

bond lengths, Å					
P-S	2.013(2)	C(6)-C(7)	1.479(7)	S-Li	2.423(8)
P-N(1)	1.699(4)	C(6)-C(8)	1.519(7)	O(1A)-Li	1.937(10)
P-N(2)	1.712(4)	N(1)-C(4)	1.459(6)	O(2A)-Li(1)	1.963(10)
P-C(6)	1.655(5)	N(2)-C(5)	1.455(6)	O(3A)-Li(1)	1.945(10)
bond angles, deg					
S-P-C(6)	115.1(2)	P-N(1)-C(4)	113.7(3)		
S-P-N(1)	111.5(2)	P-N(1)-C(1)	117.2(3)		
S-P-N(2)	107.6(6)	C(1)-N(1)-C(4)	110.8(4)		
C(6)-P-N(1)	111.1(2)	P-N(2)-C(5)	112.0(3)		
C(6)-P-N(2)	113.5(3)	P-N(2)-C(3)	118.9(3)		
N(1)-P-N(2)	96.6(2)	C(3)-N(2)-C(5)	111.0(5)		
P-C(6)-C(7)	125.3(4)	S-Li-O(1A)	110.0(6)		
P-C(6)-C(8)	117.9(4)	S-Li-O(2A)	103.3(6)		
C(7)-C(6)-C(8)	115.2(4)	S-Li-O(3A)	134.2(9)		
		P-S-Li	109.7(2)		
torsional angles, deg					
S-P-C(6)-C(7)	-15.9(6)	S-P-N(1)-C(1)	61.0(4)		
S-P-C(6)-C(8)	+179.3(4)	S-P-N(2)-C(5)	67.4(4)		
S-P-N(1)-C(4)	-70.4(4)	S-P-N(2)-C(3)	-64.2(4)		

Critical features of the crystal structure analysis are collected in Table 5, and selected bond lengths, bond angles, and torsional angles are found in Table 6. The lithium salt Li⁺5⁻ crystallizes as a tris-THF-solvated monomer (Figure 8)²³ and therein deviates from the dimeric solid state structures of the analogous *P*-benzyl 2-sulfide (Li⁺4⁻)^{6a} and the *P*-isopropyl 2-oxide (Li⁺3⁻).^{6c} The other prominent features of Li⁺5⁻ are in line with previous findings for this class of compounds: (1) lithium is coordinated to sulfur and has no carbon contact in accord with the structure found in solution by NMR analysis,^{6b} (2) the anionic carbon is nearly planar (Σ bond angles: 358.4°), (3) the carbanionic moiety is parallel to the P=S axis (S-P-C(7)-C(8): 179.3 (4)°), (4) both thio derivatives Li⁺4⁻ and Li⁺5⁻ have both their N-Me groups equatorially oriented, whereas the analogous oxo compounds show an equatorial/axial arrangement of the nitrogen substituents, and (5) the phosphorus heterocycle is in a chair conformation with the sulfide axially disposed.

The slight degree of pyramidalization at carbon is very similar for both isopropyl chalcogen analogs Li⁺3⁻ (β =

(23) There is a significant disorder in the THF molecules that leads to a modest wR2 value (0.152). The relevant part of the structure shows little variation.

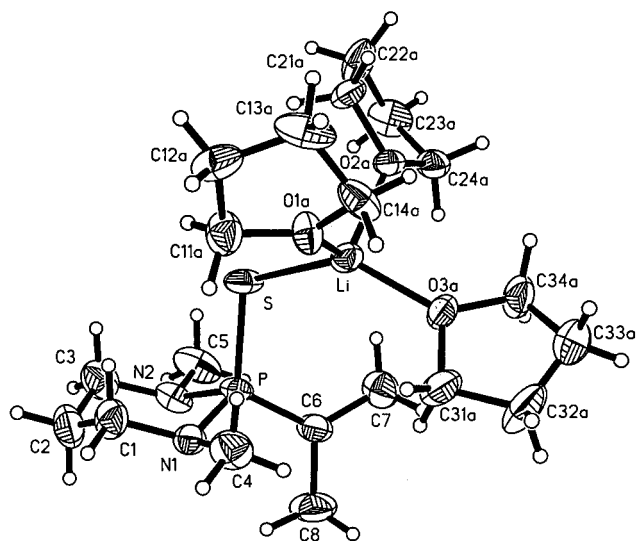


Figure 8. ORTEP plot of Li^+5^- showing 35% probability ellipsoids for non-H atoms and circles of arbitrary size for H atoms. Minor site THF positions were omitted for clarity.

97.3) and Li^+5^- ($\beta = 97.6$), but the isopropyl group is more strongly rotated around the P–C bond in Li^+3^- ($\alpha = 67^\circ$) than it is in Li^+5^- ($\alpha = 82^\circ$). This may be a consequence of the different orientation of the nitrogen substituents. A similar torsion is noted in the oxo- and thioxo-*P*-benzyl solid state structures (Li^+2^- and Li^+4^- , respectively) wherein the equatorial/axial and equatorial/equatorial disposition, respectively, has the same influence on the alignment of the carbanion with the P=X axis.

Due to the monomeric nature of Li^+5^- , the P=S bond is shorter (0.01 Å) than in the *P*-benzyl 2-sulfide (Li^+4^-) analog. The concomitant lengthening of the P–N bonds in Li^+5^- can be rationalized by the missing π acceptor (benzyl group) at the carbanion: stabilization of the negative charge occurs primarily through σ^* (P–N) orbitals, which lengthens the P–N bonds and causes the P–C bond to shorten by 0.01 Å compared to Li^+4^- . In spite of the different N–Me orientation in Li^+3^- and Li^+5^- , the P–C and P–N bond lengths are very similar which must be due to an electronic compensation through different X–P–C–C dihedral angles.

Lithio 2-Methyl-1,3,2-diazaphosphorinane 2-Oxide (Li^+12^-) and 2-Sulfide (Li^+13^-). To more closely approximate the actual chemical species, an unsolvated lithium cation has been coordinated to the chalcogen atoms of $\mathbf{12}^-$ and $\mathbf{13}^-$. The Li–X–P bond angles have been fixed at the respective X-ray values to prevent the “naked” metal from attaining spurious ring contacts and all other variables have been optimized. These structures have been depicted together with the corresponding X-ray crystallographic structures of Li^+3^- and Li^+5^- in Figures 9 and 10, respectively. Only the rotamers with the N–H’s oriented equatorially/equatorially and equatorially/axially were considered. For both chalcogens, lithium coordination lowers the relative energy of the equatorial/axial rotamer but has a more pronounced effect in the oxo (1.5 kcal/mol) than in the thioxo case (0.5 kcal/mol).²⁴ The energy ordering for the oxo case, Li^+12^- , is now reversed compared to $\mathbf{12}^-$ but is in accord with the corresponding orientation found in the solid state structure of Li^+3^- . For the sulfur derivative Li^+13^- ,

the energy ordering is the same as for the anion $\mathbf{13}^-$: the equatorial/equatorial isomer is distinctly more stable (1.5 kcal/mol) which again is in accord with the X-ray structure of Li^+5^- . This effect can be rationalized from orbital interaction considerations; the lithium cation polarizes electron density away from phosphorus by diminishing chalcogen LP back bonding. The σ^* (P–N) orbitals are thus less occupied (manifested in shorter P–N bonds) and more amenable to stabilizing an equatorial nitrogen LP.

The carbanions in all four computed structures are more strongly pyramidalized (ca. 10°) than their experimental equivalents, and the carbanions in both lowest energy structures are rotated ca. 10° further away from a parallel arrangement with the P–X axis than in both X-ray structures. Omission of solvent coordination at lithium furnishes a shorter Li–X and a longer X–P bond for both molecules compared to the corresponding values of the solid-state structures. The latter difference gives rise to less back-bonding from the chalcogens in Li^+12^- and Li^+13^- and thus shorter P–N bonds. The longer P–C bonds compared to the X-ray data must be due to the steric difference of the carbanion substituents, which is supported by the smaller C–P–X bond angles in the gas phase structures. One can regard the X-ray structures with their solvated lithiums as an intermediate species between the two computed extremes, the pure anions $\mathbf{12}^-$ and $\mathbf{13}^-$ and the molecules with unsolvated lithiums Li^+12^- and Li^+13^- . The NBO analysis generates the same picture as for the anionic species: due to less chalcogen LP back bonding in the sulfur case, stronger interaction of electron density at the carbanion and the nitrogens with the σ^* (P–N) and σ^* (P–C) orbitals is found in Li^+13^- .

Rotational Coordinates of the 2-Methyl-1,3,2-diazaphospholidine 2-Oxide ($\mathbf{14}^-$) and 2-Sulfide ($\mathbf{15}^-$) Anions. The next phase in our study was the determination of the energetic and conformational consequences of ring structure. Since many of the preparatively significant reagents incorporate a five-membered phosphorus heterocycle,²⁵ we have examined models of these species computationally. The geometries arising from incremental carbanion rotation for $\mathbf{14}^-$ and $\mathbf{15}^-$ are contained in Tables 7 and 8, respectively. In both cases, the lowest energy structure exhibits a carbanion parallel to the P=X axis ($\alpha = 90^\circ$) and pseudoequatorially oriented N–H’s. Unlike the six-ring analogs, a C_s symmetrical conformation was not found due to the staggered arrangement of the ring hydrogens. Little structural change occurs during rotation from $\alpha = 90^\circ$ to 45° . At $\alpha = 30^\circ$, however, the geometries start to differ for both molecules: in $\mathbf{14}^-$, the ethylene unit twists toward the carbanion and the N–H’s keep a staggered orientation with the respective ring hydrogens. This conformation

(24) To assure that the energy ordering for Li^+13^- and Li^+14^- is not due to the different prefixed Li–X–P angles, the oxygen analog has been reoptimized with the Li–X–P bond angle from the sulfur X-ray structure (109.7°), which had a negligible influence on the relative energies.

(25) (a) Hanessian, S.; Delorme, D.; Beaudoin, D.; Leblanc, Y. *J. Am. Chem. Soc.* **1984**, *106*, 5754. (b) Hanessian, S.; Bennani, Y. L.; Delorme, D. *Tetrahedron Lett.* **1990**, *31*, 6461. (c) Hanessian, S.; Bennani, Y. L. *Tetrahedron Lett.* **1990**, *31*, 6465. (d) Hanessian, S.; Beaudoin, S. *Tetrahedron Lett.* **1992**, *33*, 7655. (e) Hanessian, S.; Beaudoin, S. *Tetrahedron Lett.* **1992**, *33*, 7659. (f) Hanessian, S.; Gomtsyan, A.; Payne, A.; Hervé, Y.; Beaudoin, S. *J. Org. Chem.* **1993**, *58*, 5032. (g) Hanessian, S.; Bennani, Y. L.; Leblanc, Y. *Heterocycles* **1993**, *35*, 1411. (h) Hanessian, S.; Gomtsyan, A. *Tetrahedron Lett.* **1994**, *35*, 7509. (i) Hanessian, S.; Andreotti, D.; Gomtsyan, A. *J. Am. Chem. Soc.* **1995**, *117*, 10393.

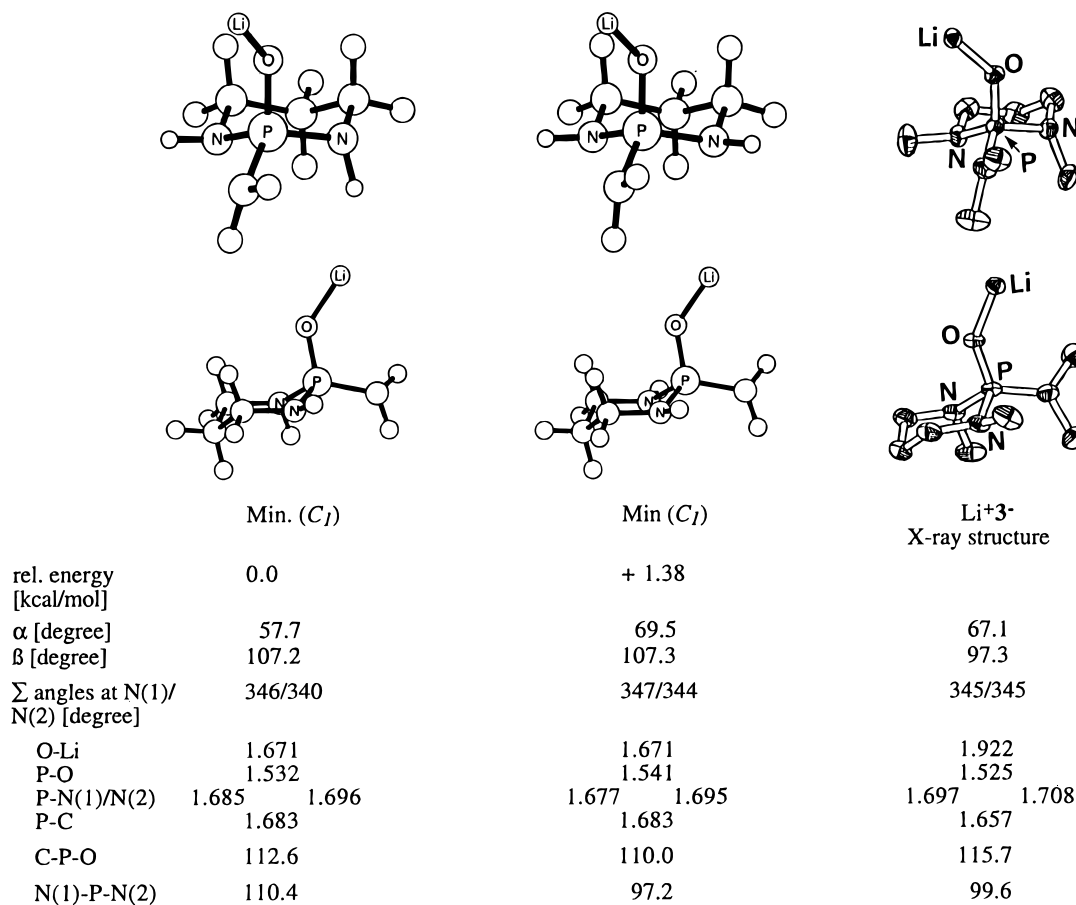


Figure 9. Stationary points for Li^+12^- at MP4(SDQ)/6-31+G*/HF/6-31+G* (Li–O–P angle fixed at 134.5°) and the X-ray structure of Li^+3^- (only half of the unit cell is shown; THF molecules and hydrogens are omitted for clarity).

of 14^- is preserved during the last two rotational increments reaching a relative energy of +8.7 kcal/mol at $\alpha = 0^\circ$.

The thioxo derivative 15^- experiences a significant change in only one of the N–H orientations at $\alpha = 30^\circ$. This nitrogen undergoes further pyramidalization, which causes its hydrogen to nearly eclipse (-9°) a hydrogen of the ethylene unit. During the next rotational step, the ethylene bridge twists toward the carbanion in a much more pronounced fashion than in 14^- , leaving both N–H's in pseudoaxial positions. At the final point of the rotational coordinate ($\alpha = 0^\circ$), one NH is again nearly eclipsed (5°) to a hydrogen of the ethylene group but the relative energy is lower (+8.7 kcal/mol) than at $\alpha = 30^\circ$. This geometry ($\alpha = 0^\circ$) is a TS (NIMAG = 1)²⁶ for the twist of the ethylene unit at HF/3-21G* but it is *not* a stationary point on the HF/6-31+G* energy surface.

Stationary Points for the 2-Methyl-1,3,2-diazaphospholidine 2-Oxide Anion (14^-). Head-on views of the four stationary points of 14^- at HF/6-31+G* along with structural parameters are given in Figure 11. As is found in five-membered carbocycles, the envelope conformation with a different atom at the flap in each of the four rotamers is adopted by 14^- . The lowest energy structure has a slightly pyramidalized carbanion whose substituents are roughly parallel to the P=O axis. Both N–H's take up pseudoequatorial orientations and are staggered with the vicinal ethylene hydrogens. The second C_1 minimum (0.7 kcal/mol higher in energy) has

a pyramidalized carbanion that is polarized to the opposite side of the ring, and one of the N–H's has moved to a pseudoaxial position eclipsing (4°) the P=O bond. The nitrogens differ considerably in their degree of pyramidalization compared to the extent found in the diazaphosphorinane 12^- . The C_s minimum (2.9 kcal/mol above the global minimum) exhibits a carbanion that is perpendicular to the P=O axis and completely sp^3 hybridized nitrogens with their hydrogens axially disposed. The TS structure for 14^- is similar to the last point ($\alpha = 0^\circ$) on the HF/3-21G* rotational coordinate: the strongly pyramidalized carbanion is perpendicular to the P=O axis, and the N–H's are oriented pseudo-equatorially/pseudoaxially. The activation energy for P–C bond rotation (+5.3 kcal/mol) is 0.6 kcal/mol lower than in 12^- .

Stationary Points for the 2-Methyl-1,3,2-diazaphospholidine 2-Sulfide Anion (15^-) and a Comparison with 14^- . The phospholidine representatives of both chalcogen families differ only in minor details (Figure 12). Both C_1 minima of 15^- are energetically nearly degenerate and exhibit a smaller deviation from each other in the orientation of the N–H's than those of 14^- . The geometry of the TS of 15^- agrees almost completely with that of the oxo analog but, as in the phosphorinanes, the relative energy is higher (2.0 kcal/mol) for the thioxo derivatives.

The ring size does not seem to have a notable effect on the geometry around phosphorus. The respective NBO charges are almost identical for both ring sizes and the NBO interactions are very similar. Stabilization of the

(26) NIMAG = number of imaginary frequencies in the Hessian matrix.

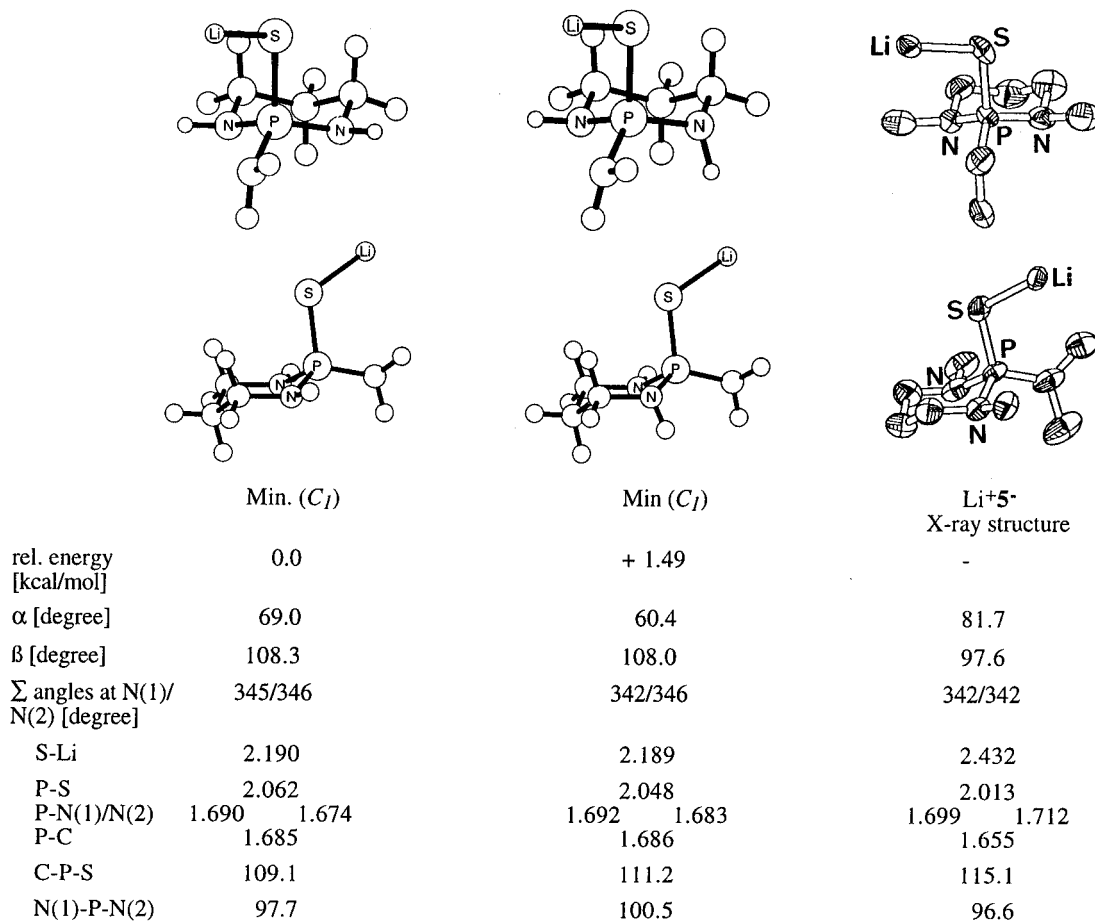
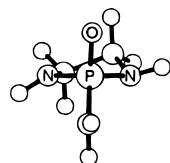


Figure 10. Stationary points for $\text{Li}^+\mathbf{13}^-$ at $\text{MP4(SDQ)/6-31+G}^*//\text{HF/6-31+G}^*$ (Li-S-P angle fixed at $109/7^\circ$) and the X-ray structure of $\text{Li}^+\mathbf{5}^-$ (THF molecules and hydrogens are omitted for clarity).

Table 7. Coordinate for the P-C Bond Rotation in $\mathbf{14}^-$ at $\mathbf{3-21G}^*$

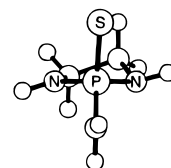


α (deg)	rel energy (kcal/mol)	β (deg)	Σ angles N(1)/N(2) (deg)
90	0.0	93.4	351/344
75	+0.20	95.6	353/341
60	+1.68	96.5	354/340
45	+4.95	95.8	352/340
30	+7.70	-91.9	342/341
15	+8.73	-102.3	339/340
0	+8.74	-105.4	337/340

negative charge in the isodesmic equation (1) $(\text{R})_2 = \text{NH}(\text{CH}_2)_2\text{NH}$ is somewhat weaker ($\text{X} = \text{O}$, -40.7 kcal/mol; $\text{X} = \text{S}$, -46.0 kcal/mol) than in $\mathbf{12}^-$ and $\mathbf{13}^-$. Only one rotamer of both $\mathbf{14H}$ and $\mathbf{15H}$ could be found computationally. The range of experimental bond characteristics²² are juxtaposed to HF/6-31+G^* -optimized values in Table 9. The computed data are well within the experimental range. In the thio derivative, one N-H is eclipsed to an ethylene hydrogen (4°). The reluctance of the hydrogens to adopt a staggered arrangement indicates the low flexibility within the phospholidine ring.

The most noteworthy feature observed during P-C bond rotation in the five-membered ring series is the strong response of the ethylene bridge. Very promising results in stereoselective reactions with phospholidine-

Table 8. Coordinate for the P-C Bond Rotation in $\mathbf{15}^-$ at $\mathbf{3-21G}^*$



α (deg)	rel energy (kcal/mol)	β (deg)	Σ angles N(1)/N(2) (deg)
90	0.0	91.8	359/343
75	+0.34	93.4	360/341
60	+2.31	94.2	360/340
45	+5.92	93.4	357/341
30	+9.96	-91.5	344/343
15	+8.20	-102.4	344/334
0	+8.68	-103.7	341/336

stabilized carbanions have been obtained with rigid auxiliaries (**iii**) in which a second ring is fused to the phospholidine at the ethylene bridge.²⁵ This bicyclic structure is conformationally rigid which results flexing of the phospholidine ring and forces both nitrogen substituents into a predetermined pseudoequatorial orientation. Since the greatest deformation is found in the TS's, it is intriguing to speculate on the energetic consequences of enforcing the GS geometry during the rotational coordinate.

The impact of this conformational bias on the energetic course of the P-C bond rotation can be computationally assessed by fixing the dihedral angles of the ethylene bridge to their ground state values and calculating the P-C rotational coordinate at HF/3-21G^* anew (Figure

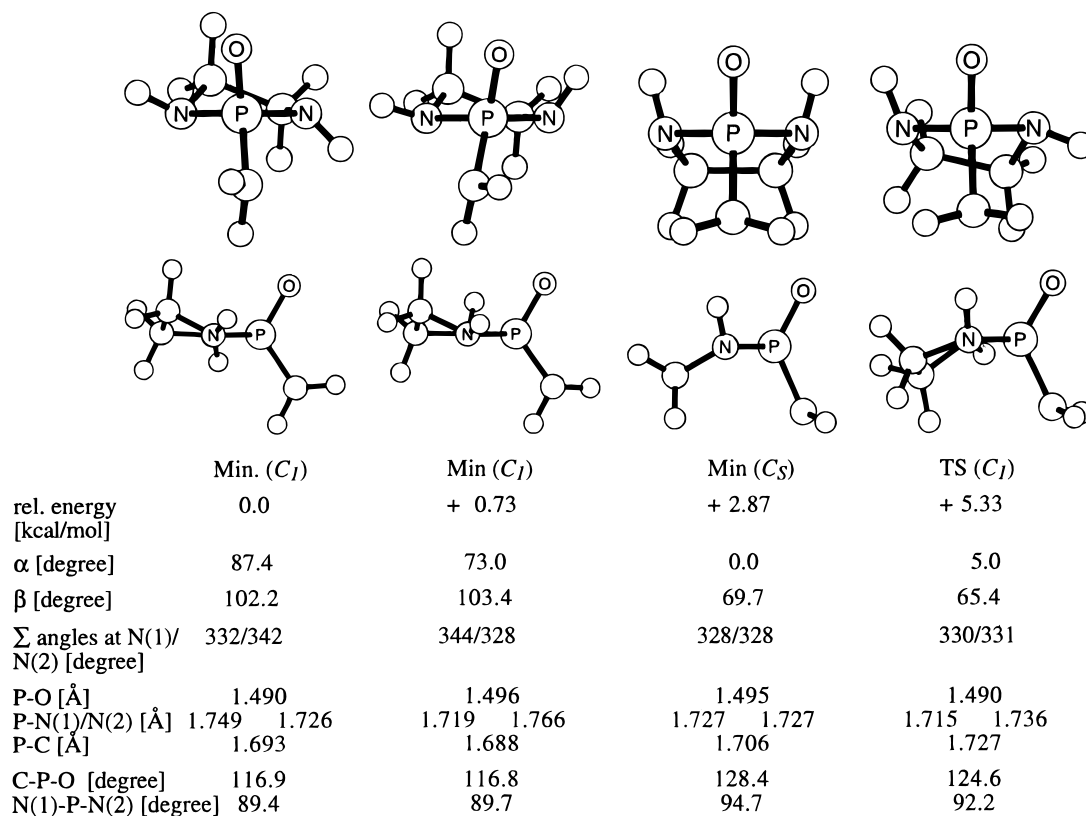


Figure 11. Stationary points for 14^- at MP4(SDQ)/6-31+G*/HF/6-31+G* (+ZPE).

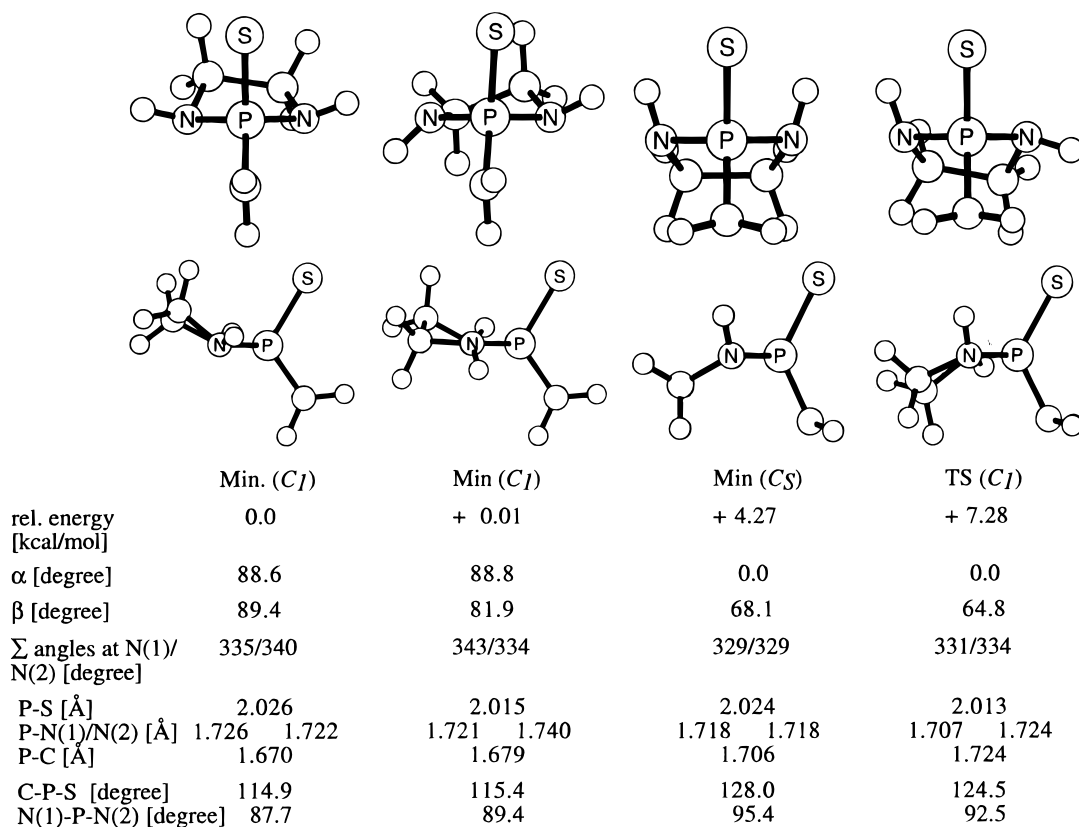
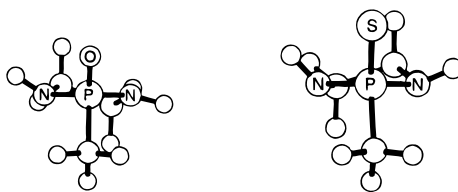


Figure 12. Stationary points for 15^- at MP4(SDQ)/6-31+G*/HF/6-31+G* (+ZPE).

13).²⁷ A steady rise in energy occurs in both rotational coordinates culminating in +11.9 kcal/mol for 14^- and +14.2 kcal/mol for 15^- at the last point ($\alpha = 0^\circ$) with the carbanion perpendicular to the P=X axis. These num-

bers are 4–6 kcal/mol higher compared to the equivalent phosphorinanes. Though this estimate cannot be taken as a quantitative measure, it may be regarded as an incentive to the design of new modifiers which increase

Table 9. Stationary Points for 14H and 15H at HF/6-31+G*


	14H	X-ray structures ^{a,b}	15H	X-ray structures ^{a,c}
	min (C ₁)		min (C ₁)	
Σ angles at N(1)/N(2) (deg)	342/353	340–359	340/341	341–360
P–X (Å)	1.465	1.45–1.48	1.954	1.93–1.96
P–N(1) (Å)	1.681	1.63–1.68	1.684	1.63–1.69
P–N(2) (Å)	1.670	1.63–1.68	1.689	1.77–1.85
P–C (Å)	1.811	1.79–1.85	1.809	1.77–1.85
C–P–X (deg)	110.5	106–110	113.1	108–116
N–P–N (deg)	92.6	93–96	94.1	104–110

^a Range of data from Cambridge Crystallographic Database. ^b Seven structures, ref 22c. ^c Seven structures, ref 22b.

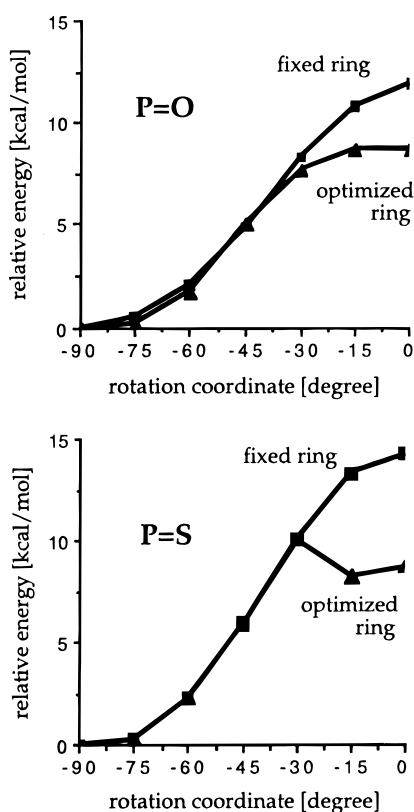


Figure 13. Energy diagram for the P–C bond rotation in **14⁻** (P=O) and **15⁻** (P=S) with an ethylene bridge fixed in the GS orientation and freely optimized.

the local dissymmetry of the anions and increase the barrier to bond rotation.

Stationary Points for the Lithio 2-Methyl-1,3,2-diazaphospholidine 2-Oxide (Li⁺14⁻) and 2-Sulfide (Li⁺15⁻). For completeness and in anticipation of an X-ray crystal structure analysis for a lithio 1,3,2-diazaphospholidine, we optimized the lithium salts of **14⁻** and **15⁻** (Table 10). The P–X–Li angles must again be fixed (vide supra) and due to a lack of experimental data, the values from Li⁺3⁻ (134.5°) and Li⁺5⁻ (109.7°) have been used.²⁸ The two structures found for both derivatives

(27) Due to the many fixed parameters in the molecules, we did not perform any higher level optimizations.

Table 10. Stationary Points for Li⁺14⁻ and Li⁺15⁻ at MP4(SDQ)/6-31+G/HF/6-31+G***

	Li ⁺ 14 ^{- a}		Li ⁺ 15 ^{- b}	
	min (C ₁)	min (C ₁)	min (C ₁)	min (C ₁)
rel energy (kcal/mol)	0.0	+1.31	0.0	+0.87
α (deg)	–70.3	67.1	–70.1	67.0
β (deg)	107.4	105.1	107.7	106.0
Σ angles at N(1)/N(2) (deg)	340/346	346/342	349/341	346/345
X–Li	1.672	1.670	2.193	2.193
P–X (Å)	1.533	1.531	2.051	2.050
P–N(1) (Å)	1.707	1.682	1.677	1.699
P–N(2) (Å)	1.685	1.709	1.704	1.683
P–C (Å)	1.683	1.683	1.683	1.683
C–P–X (deg)	109.7	109.6	109.1	109.0
N–P–N (deg)	91.2	91.1	91.1	91.0

^a Li–O–P angle fixed at 134.5°. ^b Li–S–P angle fixed at 109.7°.

display the same orientation of the ring conformation and of the nitrogen substituents and differ only in the disposition of the deprotonated carbon and the metal. The nitrogen substituents are staggered with the ring methylenes and the lone pair at carbon is directed towards lithium. Surprisingly, the orientation of the nitrogen substituents relative to the carbanion/cation moiety in both *higher* energy structures corresponds to the same arrangement in the respective 6-membered ring analogs. The close similarities in geometric parameters between both ring series (apart from the N–P–N angles) is noteworthy.

The energy differences between the geometries of Li⁺14⁻ (1.3 kcal/mol) and of Li⁺15⁻ (0.9 kcal/mol) are only slightly lower than those in the six-membered ring analogs. The good correspondence between solid state and computed structures in the latter examples tempts us to expect a similar agreement for the 5-membered ring series. Efforts along these lines are in progress.

Conclusion

The computed lowest energy structure of the 2-methyl-2-oxo- and -2-thioxophosphorinane anions exhibit carbanion substituents parallel to the P=X axis (X = O, S) in accord with solution (NMR) and solid state (X-ray crystal structure) findings. The X-ray crystal structure analysis of a monomeric lithiated phosphorus-stabilized carbanion further supports the orientational preferences elucidated by computation. The difference in the experimental N-substituent orientation between the oxo and the thio derivative is also found in the computed anions and even more so in the optimizations including the lithium cation. The TS structures for P–C bond rotation display pyramidalized carbanions with the substituents oriented pseudoperpendicularly to the P=X bonds. The experimentally measured (NMR) higher P–C rotational barrier for the thio analog is quantitatively reproduced in these calculations.

Thermochemical stabilities (isodesmic equations), favorable orbital interactions (NBO analysis), and bond length comparisons indicate a stronger GS stabilization through P–S than P–O. The latter two indicators also

(28) A larger value for the P–O–Li compared to the P–S–Li angle is also found in the X-ray structures of the lithio *P*-benzyl derivatives (Li⁺2⁻, 140.2°; Li⁺4⁻, 111.2°). This is a general trend in coordination compounds with these phosphine chalcogens: Burford, N.; Royan, B. W.; Spence, R. E. v. H.; Rogers, R. D. *J. Chem. Soc., Dalton Trans.* **1990**, 2111.

strongly hint to a superior TS stabilization through P–O. Both effects act in concert to yield the higher P–C rotational barrier in the sulfur analog.

The 2-methyl-2-oxo- and -2-thioxophospholidine anions show the same conformational characteristics and bonding patterns around phosphorus (i.e., higher P–C rotational barrier for the thioxo analog) but differ substantially in the strong orientational response of the ring system to P–C bond rotation.

Acknowledgment. We wish to thank the National Institute of Health (PHS R01 GM45532) for financial support. This work was partly supported by the Na-

tional Center of Supercomputing Applications, University of Illinois at Urbana–Champaign under Grant Nos. CHE940009N and CHE950005N.

Supporting Information Available: Archive entries of all HF/6-31+G* optimizations are provided (34 pages). This material is contained in libraries on microfiche, immediately follows this article in the microfilm version of the journal, and can be ordered from the ACS; see any current masthead page for ordering information.

JO9602783